



**HAL**  
open science

## The use of CPT based metamodels to predict the performance of offshore anchor piles

Alessio Mentani, Laura Govoni, Franck Bourrier

### ► To cite this version:

Alessio Mentani, Laura Govoni, Franck Bourrier. The use of CPT based metamodels to predict the performance of offshore anchor piles. Cone Penetration Testing 2022, Jun 2022, Bologna, Italy. pp.1016 - 1022, 10.1201/9781003308829-153 . hal-04700969

**HAL Id: hal-04700969**

**<https://hal.science/hal-04700969v1>**

Submitted on 18 Sep 2024

**HAL** is a multi-disciplinary open access archive for the deposit and dissemination of scientific research documents, whether they are published or not. The documents may come from teaching and research institutions in France or abroad, or from public or private research centers.

L'archive ouverte pluridisciplinaire **HAL**, est destinée au dépôt et à la diffusion de documents scientifiques de niveau recherche, publiés ou non, émanant des établissements d'enseignement et de recherche français ou étrangers, des laboratoires publics ou privés.



Distributed under a Creative Commons Attribution - NonCommercial - NoDerivatives 4.0 International License

# The use of CPT based metamodels to predict the performance of offshore anchor piles

A Mentani & L. Govoni

*University of Bologna, Bologna, Italy*

F. Bourrier

*French National Research Institute for Agriculture, Food and Environment, Grenoble, France*

**ABSTRACT:** The paper presents the development of metamodels for the prediction of the load-displacement response of steel piles driven in sand subjected to pull-out. Two metamodels are created for the evaluation of the tensile capacity and initial stiffness of the pile. They were developed based on the outcomes of a finite element testing campaign, employing models of parameters derived from the tip resistance of cone penetration tests. Two hundreds finite element simulations, which included various soil-pile configurations, were required to calibrate accurate metamodels. Assessment of the procedure was carried out with reference to available data on a model pile and related cone penetration test results. The approach relies on particularly simplified finite element models, but it can be extended to accommodate modelling features of higher complexity. The results find application to the design of offshore piles used as anchors for floating structures.

## 1 INTRODUCTION

The paper focuses on the drained, static load-displacement response of steel open-ended piles subjected to pull-out. In the offshore environment, tensile loading conditions may become critical for piles employed as anchor foundations, particularly when used with vertical or taut line moorings. In the context of offshore wind exploitation, these solutions offer an attractive alternative to catenaries, as they may allow to contain the area over which a floating wind farm would extend, aiding with a reduction of the investment costs (Castro-Santos & Diaz-Casas 2016).

The tensile response of offshore piles is traditionally estimated using the shaft load-transfer curve approach, combined with ultimate shaft friction prediction methods. The development of load-transfer curves dates back to the Fifties and several formulations are now available as comprehensively reviewed in Bohn et al. (2017). In sand, the tensile capacity is now estimated according to cone penetration test-based procedures (CPT-methods), which predictive performance was assessed in Schneider et al. (2008). The approach is very accurate and its implementation straightforward, however, uncertainties may arise when selecting the most suitable formulation among those available (Foglia et al. 2017, Schmoor et al. 2018).

Finite element or finite difference models can be also employed to describe the pile tensile load-

displacement curve (De Nicola & Randolph 1993; van Tol & Broere 2006; De Gennaro et al. 2008).

The implementation and calibration of these models can be, however, a complex and computationally onerous task. To overcome this limitation, metamodelling techniques can be employed, as they allow to store the results of finite element analyses in simple mathematical functions, which have the advantage of an easy implementation and low computational cost (Sudret 2008).

In this paper, metamodels are developed to predict some behavioural features of piles driven in a homogeneous sand bed. Building up on the experience matured in the context of the CPT-methods over the last decade, a simple CPT-based Finite Element (FE) modelling strategy is adopted to investigate the pile response when subjected to a tensile load through a parametric study. A Polynomial Chaos Expansion (PCE) metamodel (Xiu & Karniadakis 2002) is built from the results obtained by the FE study. The prediction capacity of the developed metamodel is then assessed with respect to selected data included in the ZJU-ICL experimental database of piles driven in sand (Yang et al. 2015).

## 2 FE SIMULATION PROGRAMME

A FE parametric study was carried out, in which an upward vertical displacement was applied to

a wished in place model pile. They were total stress, small-strain and static analyses and the software suite Abaqus FEA (ABAQUS 2014) was used to the scope.

## 2.1 Details of the FE models

The FE models used in the parametric study involved a pile foundation of diameter  $D$ , length  $L$  and wall thickness  $t$ . The pile is subjected to a drained axial pull-out test from a uniform sand deposit, that is characterised by a constant value of the relative density  $D_r$ , and a constant effective unit weight ( $\gamma' = 10 \text{ kN/m}^3$ ). The models were axial-symmetric, with zero displacement boundaries set at a distance of  $15D$  from the pile shaft and  $10D$  down the pile tip. A sensitivity study was carried out which showed that, to avoid any convergence issues, a very fine uniform mesh was required in the vicinity of the pile (Figure 1).

Assuming a fully plugged failure, the pile was modelled as a solid, deformable element, obeying to a linear elastic constitutive law. It features a uniform cross section. The equivalent density and elastic properties were calculated to account for the section geometry on the pile weight and axial deformation.

The soil response was modelled as linear-elastic and perfectly plastic, failing according to the Mohr-Coulomb criterion. Model parameters are derived from an artificial cone tip resistance ( $q_{c,FE}$ ). The particular form of the trend is generated according to the relation given by Jamiolkowski et al. (2003) as this was also used in the interpretations made in the ZJU-ICL database (Yang et al. 2015).

$$q_{c,FE} = 20 \cdot \exp\left(\frac{D_r}{0.35}\right) \cdot p_a \cdot \left(\frac{\sigma'_{v0}}{p_a}\right)^{0.5} \quad (1)$$

where  $p_a$  = atmospheric pressure and  $\sigma'_{v0}$  = in situ vertical effective stress.

The soil's Young modulus was prescribed to vary with the artificial cone tip resistance according to Robertson (2009)

$$E' = \alpha_E \cdot q_{net,FE} \quad (2)$$

where

$$\alpha_E = 0.015 \cdot (10^{0.55I_c + 1.68}) \quad (3)$$

applies to the net tip resistance and  $I_c$  = soil behaviour type index. Soil peak strength and dilation angles were implemented in the FE models according to well-established Bolton (1986) correlation. The critical state interface friction angle was taken constant ( $\delta_{cv} = 29^\circ$ ), as it is generally done for steel driven piles in case interface tests are not available

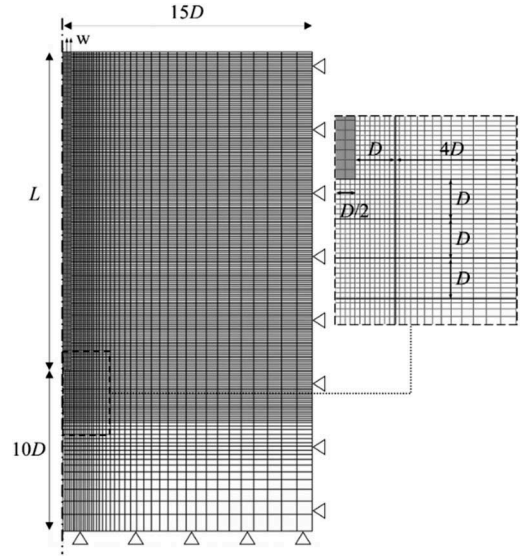


Figure 1. Distribution of the mesh size along the FE models geometry and applied boundary conditions.

(Schneider et al. 2008). Piles were wished in place, therefore the effects of installation on the soil stress state prior to loading was implemented to ensure that the radial stress on the pile was, at any soil depth, that predicted by Jardine et al. (1998)

$$\sigma'_h = 0.029 \cdot q_{c,FE} \cdot \left(\frac{\sigma'_{v0}}{p_a}\right)^{0.13} \cdot \left(\frac{L-z}{R^*}\right)^{-0.38} \quad (4)$$

where  $R^* = 0.25 \cdot [D^2 - (D - 2t)^2]^{0.5}$ .

## 2.2 Sampling and results

Five independent input variables were considered in the design of the FE test programme. The pile was described by three variables, whose range was established to encompass the geometries encountered in the ZJU-ICL experimental database. Two variables were used for the definition of the soil model: the relative density and the modulus factor,  $\alpha_E$ , which were

Table 1. Input variables for the FE test programme.

| Input variable                      | Range       |
|-------------------------------------|-------------|
| Pile diameter $D$ [m]               | 0.20 – 1.00 |
| Pile slenderness $L/D$ [-]          | 10 – 70     |
| Pile wall thickness ratio $D/t$ [-] | 10 – 100    |
| Soil density $D_r$ [%]              | 40 – 100    |
| Soil modulus factor $\alpha_E$ [-]  | 3 – 10      |

allowed to vary within a realistic range for clean sands (i.e.,  $I_c = 1.31 - 2.05$ ). All the input variables are collected in Table 1, along with their domain of variation.

The FE analyses were conducted with certain combination of the input variables by using the Latin Hypercube Sampling technique (LHS, McKay et al. 1979). According to the LHS, each input variable range is divided into intervals of equal probability. The number of intervals is equivalent to the sample dimension and the location of the design point (i.e. the combination of inputs) is taken randomly within the interval. This method allows for an optimum coverage of the input variable domain and the sample size can be easily increased.

In this study, the five input variables were first combined to create a LH sample of size 50 ( $S_{50}$ ), which was increased to 100 ( $S_{100}$ ) and then to 200 ( $S_{200}$ ). In Figure 2, the results of the 200 simulations are shown in terms of normalised vertical force ( $V/(\gamma'DL^2)$ ) and displacement ( $w/D$ ). Two outputs variables were identified along the curves, the normalised tensile capacity ( $V_{ult}/(\gamma'DL^2)$ ) and the normalised initial stiffness ( $K_i/(\gamma'L^2)$ ), which was evaluated as the initial tangent to the curve.

The input combinations and the resulting outputs were then used for the development and calibration of the PCE metamodels. To validate the metamodels further FE analyses were performed on a new sample of size 50 ( $S_{val}$ ).

### 3 DEVELOPING METAMODELS

A metamodel (MM) or surrogate model is the model of a model, and metamodeling is the process of generating such MMs. A metamodel is an explicit mathematical algorithm representing the relation between input

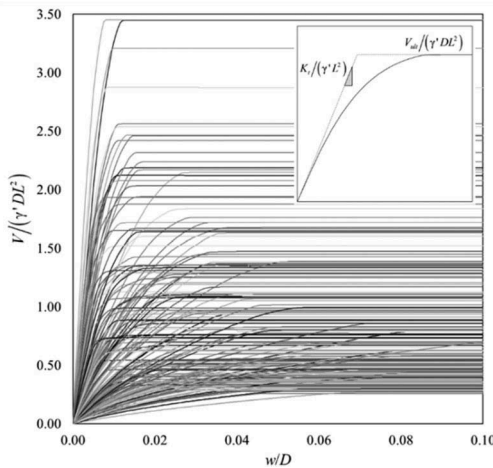


Figure 2. Results of the FE test programme in terms of dimensionless force and displacement.

and output variables and it approximates the complex and implicit function defined by the emulated model (this model is either deterministic or random). They are generally grouped into classification and regression types. When the aim is to predict a continuous target variable, as in the case examined in this paper, the regression type, such as the PCE, is to be used. In this work, the open-source Python package OpenTURNS (Baudin et al. 2016) was used to build the MMs.

#### 3.1 Details of the PCE

A given model is described by a vector  $\mathbf{X}$  in which a finite number of input random variables are gathered. The response vector  $\mathbf{Y}$ , which collects the output quantities, can be represented as the application of a mathematical model to the input vector. The PCE is an algorithm which approximate this function, and the chaos representation of the response vector is defined as the linear combination of selected multivariate orthonormal basis,  $\Psi_k(\mathbf{Z})$ , and their corresponding coefficient  $\alpha_k$  as represented by

$$\mathbf{Y} = f(\mathbf{X}) \approx \hat{f}(\mathbf{X}) = \sum_{k \in K} \alpha_k \Psi_k(\mathbf{Z}) \quad (5)$$

with  $\mathbf{Z}$  obtained by applying an isoprobabilistic transform to the input vector ( $\mathbf{Z} = \mathbf{T}(\mathbf{X})$ ).

The choice of the family of orthonormal basis (e.g., Legendre, Hermite, Krawtchouk) depends on the distribution type of the input variables, which are rescaled by the isoprobabilistic transform into common distribution types (e.g., uniform, normal, binomial). The following step consists on the determination of the coefficients,  $\alpha_k$ , associated to each polynomial basis. These coefficients are estimated according to a suitable regression strategy (Sudret 2008). The most common are the least squares strategy that minimise the quadratic error between the model response and the polynomial approximation, and the integration strategy, which uses the inner product rules, thanks to the orthogonality and normality property of the polynomial basis.

#### 3.2 Calibration and validation of the PCE

Two MMs were calibrated using the results of the FE test programme as follows. The combinations of the five input variables listed in Table 1 were collected in the input vector  $\mathbf{X}$ , and the selected outputs (i.e., the normalised pile tensile capacity load and tangent initial stiffness) represented two response surfaces (i.e.,  $\mathbf{Y}$ ). A uniform distribution of the input variable was selected as the most suitable to be applied to sample created with the LHS technique. Consequently, the Legendre orthonormal polynomial basis were chosen as associated to this distribution type. As for the evaluation strategy to compute the

polynomials coefficients, the least squares method was selected as it was shown to provide more accurate results, if compared to the integration strategy.

The calibration (i.e. the identification of coefficient  $\alpha_k$ ) of the two MMs was carried out using the results of the FE test programme originated by the created samples ( $S_{50}$ ,  $S_{100}$ ,  $S_{200}$ ). Accordingly, three MMs ( $MM_{50}$ ,  $MM_{100}$ ,  $MM_{200}$ ) were created for each of the two outputs ( $V_{ult}/(\gamma' DL^2)$ ,  $K_T/(\gamma' L^2)$ ) to explore the influence of the sample size on their accuracy. To the aim, the validation set of input-output combinations ( $S_{val}$ ) was used, with the predictive coefficient,  $Q^2$ , defined by

$$Q^2 = 1 - \frac{\sum_{l=1}^N (Y_l - \hat{f}(X_l))^2}{Var(Y)} \quad (6)$$

where  $N$  is the size of the validation sample ( $N=50$ ) and  $Var(Y)$  is the variance of the FE model outputs.

The MMs predictions are compared with the results of the FE testing campaign with reference to the two considered outputs: the tensile capacity (Figure 3a) and the initial stiffness (Figure 3b). Different markers are used to identify the MM's predictions built on different sample sizes. Some scatter is observed in the prediction of MM calibrated with the smaller sample size ( $MM_{50}$ ), particularly at low and high output values and this is particularly evident for the prediction of the tensile capacity. The increase in the sample size, reduces the error at either end of the output distribution, with  $MM_{200}$  ensuring an excellent accuracy, consistent for both the outputs and estimated to be larger than 0.98.

## 4 ASSESSMENT OF THE PROCEDURE

### 4.1 Experimental data

The data used to explore the approach potential as a predictive tool were selected among those available in ZJU-ICL experimental database. The database was developed with the scope of validating the CPT-methods for axial pile capacity. Therefore, the results of the pile loading tests are always accompanied by the relevant CPT tip resistance profiles.

Among all, the data of a pile subjected to pull-out was chosen. The selection was made to ensure that the foundation and the soil had characteristics consistent with the FE models used in the calibration procedure and that are describable through the proposed set of input. The adopted pile was steel, open-ended driven, the soil was uniform, dense, fine to medium flandrian marine sand. The  $q_c$  profile at the test location is shown in Figure 4a.

The  $q_c$  data were processed to estimate the relative density at the pile location according to equation

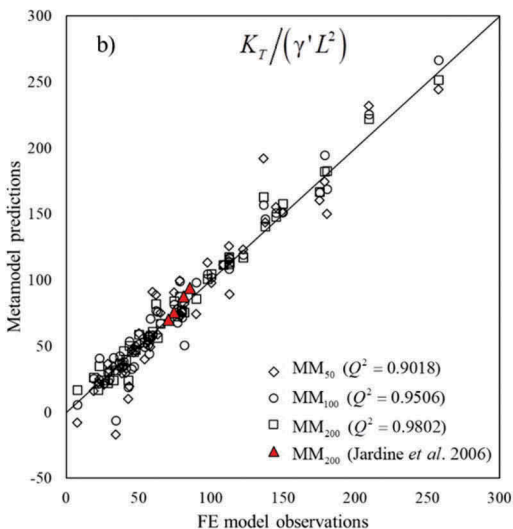
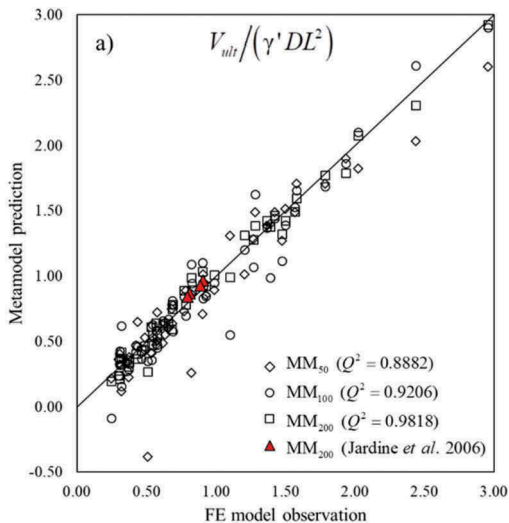


Figure 3. Accuracy of the MMs in predicting: (a) the tensile capacity; (b) the initial stiffness.

1. For a further and likely estimate of the results, the expression suggested by ISO standards (ISO, 2016) for the implementation of the CPT-methods was also employed

$$D_r = \frac{1}{2.96} \cdot \ln \left( \frac{q_c/p_a}{24.94 \cdot (p'_m/p_a)} \right)^{0.46} \quad (7)$$

where  $p'_m$  = effective mean in situ stress.

The profiles of relative density estimated with equations 1 and 7 are shown in Figure 4b, along with their average values. Application of equation 1

to the two average relative density values returns the artificial tip resistance profiles inserted in Figure 4a, which are implemented in the FE models according to the procedure described in section 1.1.

Table 2 collects the input data used for the FE and MMs. These includes the experimental pile geometry, the average relative densities, and two values of  $\alpha_E$ , corresponding to possible upper and lower bound for  $I_c$ , estimated using the information on the test site available in Jardine et al. (2006).

Table 2. Input data for FE and MM.

| $D$ [m] | $L/D$ [-] | $D/t$ [-] | $D_r$ [%]    | $\alpha_E$ [-] |
|---------|-----------|-----------|--------------|----------------|
| 0.457   | 42.23     | 33.8      | 72.04; 76.25 | 5              |
|         |           |           | 72.04; 76.25 | 7              |

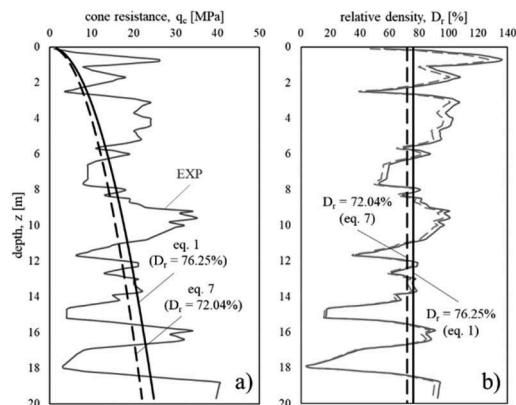


Figure 4. a) CPT data at the pile test location (redrawn from Yang et al. 2015 and artificial profile): (a) evolution of the cone resistance  $q_c$  and (b) relative density  $D_r$  depending on depth.

#### 4.2 FE models and MM prediction

The data in Table 2 were employed first to assess the FE strategy presented in section 1.1. This validation plays a crucial role in the development of MMs, as their performance relies upon the robustness of the mechanical models they stem from.

Four FE analyses were performed (as detailed in Table 2) and the results are shown to compare well with the experimental data in terms of load-displacement curves (Figure 5). A close approximation of the initial stiffness and non-linearity prior to failure are observed, with the experimental capacity falling in the rather narrow band defined by the results obtained with the two sets of FE simulations performed with the two different estimates of relative density. The average FE capacity is 1443 kN, very close to the experimental data (1450 kN). The initial

experimental stiffness (about 380 MN/m) is slightly underestimated by the FE models, which predicted an average value of 310 MN/m and 270 MN/m with  $\alpha_E$  equal to 5 and 7, respectively. A better fit could be obtained with a larger value of the modulus factor.

To assess the ability of the MM to reproduce the experimentally observed behaviour, the most accurate MMs were used (MM<sub>200</sub>). The predictions for the different input combinations of Table 2 are inserted in Table 3.

These results are compared with those predicted with the FE models in Figure 3 (triangular markers), showing consistency of the MM<sub>200</sub> accuracy. Combining the outputs of the two MMs a bi-linear response can be drawn and a direct comparison with the experimental load-displacement curve can be pursued, as depicted in Figure 6. As the MMs were built to predict selected behavioural features, they were not expected to capture the entire curve, but to provide a good estimation of the initial experimental stiffness and tensile capacity. Capacity values well compared with the results of API and NGI methods: 1450 kN and 1559 kN, respectively. A slightly higher estimate was observed when compared to the prediction of the UWA, ICP and Fugro approaches, respectively 1304 kN, 1310 kN and 1100 kN.

The results were obtained using a very simplified FE strategy and produced encouraging results. A better implementation of the  $q_c$  profile as input

Table 3. Predictions of MM<sub>200</sub>.

| Outputs        | $D_r = 72\%$ ; | $D_r = 72\%$ ; | $D_r = 76\%$ ; | $D_r = 76\%$ ; |
|----------------|----------------|----------------|----------------|----------------|
|                | $\alpha_E = 5$ | $\alpha_E = 7$ | $\alpha_E = 5$ | $\alpha_E = 7$ |
| $V_{ult}$ [kN] | 1597           | 1478           | 1641           | 1433           |
| $K_t$ [MN/m]   | 350            | 326            | 280            | 261            |

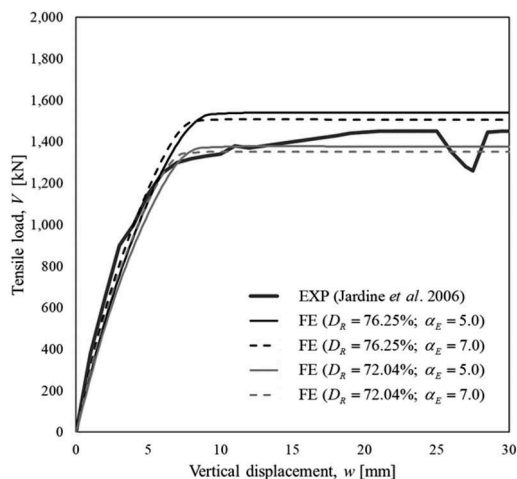


Figure 5. Experimental and FE load-displacement curves.

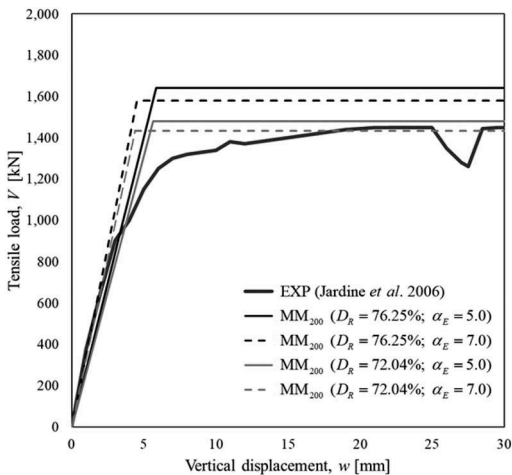


Figure 6. Experimental and MM<sub>200</sub> load-displacement curves.

variable should be pursued for a more reliable procedure. A possible way could be to follow the approach recently proposed by Cai et al. 2021.

## 5 CONCLUDING REMARKS

The paper has presented the development of a novel procedure for the prediction of the tensile response of steel displacement piles in sand. The approach has made use of a metamodeling technique, employed to store the results of a FE test programme with the aim of make them available for preliminary design purposes.

The FE models were simple, with soil parameters easily identifiable from CPT results. The modelling choices largely relied on the recent advance in the prediction of the axial capacity of offshore piles in sand with the CPT-based methods, thanks to which, available empirical correlations, had been validated on a large database of model tests.

The results obtained, although preliminary, have shown that:

- a simple CPT-based FE modelling strategy can produce results which compare well with experimental data, encouraging further validation;
- MMs can be built using a relatively small number of FE simulations and provide very accurate results over wide domains of input variables;
- inputs of MMs can be easily identified based on the interpretation of CPT data and produces good estimate of the experimental response.

Overall, the implementation of MMs is rather straightforward, avoiding the laborious FE modelling activities. MMs also run at a negligible

computational cost and are therefore suitable to parametric studies, which can be, in turn, interpreted in a probabilistic framework. The procedure, here presented in its essential steps, can be further extended to accommodate modelling features of higher complexity, increasing the number of input variables and can be employed to predict other behavioural aspects, increasing the numbers of outputs.

## ACKNOWLEDGEMENT

This work forms part of the activities of the project SEAFLOWER, which has received funding from the European Union's Horizon 2020 research and innovation programme, under the Marie Skłodowska-Curie grant agreement No 891826.

## REFERENCES

- ABAQUS 2014. Analysis User's Manual. Version 6.14, Dassault Systemes Simulia, Inc.
- Baudin, M., Lebrun, R., Iooss, B., Popelin, A-L. 2016. OpenTURNS: an industrial software for uncertainty quantification in simulation. In R. Ghanem, D. Higdon & H. Owhadi (eds.) *Handbook of uncertainty quantification*. Springer International Publishing.
- Bohn, C., Lopes dos Santos, A., Frank, R. 2017. Development of axial pile load transfer curves based on instrumented load tests. *Journal of Geotechnical and Geoenvironmental Engineering* 143 (1):04016081.
- Bolton, M.D. 1986. The strength and dilatancy of sands. *Geotechnique* 36(1): 65–78.
- Castro-Santos, L. & Diaz-Casas, V. 2016. *Floating Offshore Wind Farms*. Switzerland: Springer International Publishing.
- Cai, Y., Bransby, F., Gaudin, C., Uzielli, M. 2021. A framework for the design of vertically loaded piles in spatially variable soil. *Computers and Geotechnics* 134: 104140.
- Foglia, A., Wefer M., Forni, F. 2017. *Large-Scale Experiments and Load Transfer Analysis of Piled Foundations Supporting an Offshore Wind Turbine*. Offshore Site Investigation Geotechnics, 8th International Conference Proceeding, pp. 1078-1083(6).
- De Nicola, A. & Randolph, M.F. 1993. Tensile and compressive shaft capacity of piles in sand. *Journal of Geotechnical Engineering* 119(12): 1952–1973.
- De Gennaro, V., Frank, R., Said, I. 2008. Finite element analysis of model piles axially loaded in sands. *Rivista Italiana di Geotecnica* 2: 44–62.
- ISO (International Organization for Standardization) 2016. 19901-4: Petroleum and natural gas industries – specific requirements for offshore structures. Part 4: Geotechnical and foundation design considerations. Geneva, Switzerland.
- Jamiolkowski, M.B., Lo Presti, D.F.C., Manassero, M. 2003. Evaluation of relative density and shear strength of sands from CPT and DMT. *Soil Behaviour and Soft Ground Construction. ASCE, Geotechnical Special Publication* 119: 201–238.
- Jardine, R.J., Overy, R.F., Chow, F.C. 1998. Axial capacity of offshore piles in dense North Sea sands. *Journal of Geotechnical and Geoenvironmental Engineering* 124 (2): 171–178.

- Jardine, R.J., Standing, J.R. & Chow, F.C. 2006. Some observations of the effects of time on the capacity of piles driven in sand. *Géotechnique* 56(4): 227–244.
- McKay, M.D., Beckman, R.J., Conover, W.J. 1979. A comparison of three methods for selecting values of input variables in the analysis of output from a computer code. *Technometrics* 21(2): 239–245.
- Robertson, P.K. 2009. Interpretation of cone penetration tests – a unified approach. *Canadian Geotechnical Journal* 46: 1337–1355.
- Schmoor, K.A., Achmus, M., Foglia, A., Wefer, M. 2018. Reliability of design approaches for axially loaded offshore piles and its consequences with respect to the North Sea. *Journal of Rock Mechanics and Geotechnical Engineering* 10(6): 1112–1121.
- Schneider, J.A., Xiangtao, X., Lehane, B. 2008. Database assessment of CPT-based design methods for axial capacity of driven piles in siliceous sands. *Journal of Geotechnical and Geoenvironmental Engineering* 134(9): 1227–1244.
- Sudret, B. 2008. Global sensitivity analysis using polynomial chaos expansions. *Reliability Engineering and System Safety* 93: 964–979.
- van Tol, A.F. & Broere, W. 2006. Modelling the bearing capacity of displacement piles in sand. *ICE Proceedings Geotechnical Engineering* 159(3): 195–206.
- Xiu, D. & Karniadakis, G.E. 2002. The Wiener-Askey Polynomial Chaos for stochastic differential equations. *SIAM Journal on Scientific Computing* 24(2): 619–644.
- Yang, Z.X., Jardine, R.J., Guo, W.B., Cow, F. 2015. A new and openly accessible database of tests on piles driven in sands. *Géotechnique Letters* 5: 12–20.